Analyst

Accepted Manuscript

ROYAL SOCIETY OF CHEMISTRY

www.rsc.org/analyst

Analysis of the effects of dietary fat on body and skin lipids of hamsters by Raman spectroscopy

Phiranuphon Meksiarun, Yui Maeda, Tatsuya Hiroi, Bibin B. Andriana, and Hidetoshi Sato*

Department of Bioscience, School of Science and Technology, Kwansei Gakuin University, Gakuen, Sanda, Hyogo, 669-1337, Japan

*Corresponding author,

Phone & Fax: +81-79-565-7228; E-mail address: hidesato@kwansei.ac.jp

Abstract

Raman spectroscopy has previously been applied for studying lipid metabolism. In this study, a ball lens-installed hollow optical fiber Raman probe (BHRP) was used for the noninvasive measurement of skin lipids in hamsters. Our analysis suggested that multi-unsaturated lipids, once converted into a structure containing conjugated double bonds, were oxidized into form peroxides. These results were applied for analyzing lipid metabolism in adipose and skin tissues in hamsters fed tricaprin, saturated medium-chain triglycerides and trilinolein, unsaturated long-chain triglycerides fat diets. Unsaturated lipids formed conjugated structures in skin tissue but not in adipose tissue. Principal component analysis (PCA) revealed that the dietary fat intake correlated strongly with lipid composition in body and skin tissues. Hence, the present results successfully demonstrate that Raman spectroscopy with a BHRP can be a powerful tool for analyzing lipid metabolism.

Key words: Raman spectroscopy, fiber optic Raman probe, skin lipids, non-invasive

Introduction

FAO recently addressed the challenge of preventing and controlling non-communicable diseases (NCDs) in its 2014 global forum. NCDs including diabetes, heart disease, and cancer, are among the leading causes of death globally. One of the leading factors accounting for NCDs is obesity. The major cause of obesity is an unhealthy or high-fat diet. A study conducted from 1990 to 2010 revealed that the global body-mass index increased continuously over this period.[1] Several studies have suggested that a reduction in saturated fat (e.g. butter or margarine) intake, with a concomitant shift to unsaturated fat consumption (e.g. olive oil and fish oil) reduced LDL cholesterol and postprandial blood glucose levels, consequently lowering the risk of heart disease. [2,3] However, not all trans-fat is culpable for obesity-linked diseases. For example, tricaprin (TC), having trans-medium chain fatty acids (MCFA) found abundantly in milk fat and coconut oil, is beneficial in increasing high-density lipoprotein levels.[4] Dietary fats are generally long-chain triglycerides (TGs) with long chain fatty acid (LCFA) chains which has 14 or more carbon atoms. In contrast, medium-chain TGs are composed of MCFAs with 8 or 10 carbons. They are metabolized differently.[5] MCFAs are highly susceptible to breakdown as a "ready-to-use" fat. These facilitate oxidation reactions in the liver and release energy more readily.[5-7] Trilinolein (TL), having unsaturated LCFAs, has also been reported for its beneficial effects as a mediator of inflammatory responses, and for maintaining healthy skin conditions.[8] Thus, the metabolism of fats with different chain length and saturation attracts keen attentions of researchers.[9]

In the present study, we applied Raman spectroscopy for the study on the fat metabolism. Raman spectroscopy had been successfully applied for studies of the skin of which ranging from thickness of the stratum corneum to the effects of skin lipid content on aging.[10-12] Subcutaneous

adipose tissue isolated from different species (pigs, chickens, sheep, and cows) have been used to classify the fat-type and predict the amount of fatty acid with 99.6% and 80%–97% accuracy respectively.[13,14] Muik et al. reported the lipid degradation in vegetable oil using Fourier transform (FT-) Raman spectroscopy.[15] Their results demonstrated the feasibility of Raman spectroscopy to detect the changes in 6 vegetable oils with varied unsaturated fatty acid heated to 160°C. The conjugated diene moiety was reported as a marker for early stage of lipid oxidation. A ball lens-installed hollow optical fiber Raman probe (BHRP) would be a powerful tool for analysis of fat content in the skin.[16,17] In the previous report, BHRP successfully detected colorectal tumor advancement in live animals.[18]

Here, we aimed to evaluate the relationship between dietary fat and skin lipids at the molecular level using the Raman analysis. The metabolic and digestive reactions for LCFA and MCFA function through different pathways and have different endpoints. For example, TL which possesses three LCFAs, passes through the lymphatic system and is stored mainly in adipose tissue.[5,6] Most part of the MCFA are transported via the portal vein to be oxidized in the liver while small portions are packed together with LCFA in chylomicrons which is a lipoprotein transporting lipids in lymphatic vessels.[19]

In the present study, we demonstrate the potential of Raman spectroscopy in a real time, in situ analysis of fat accumulation in the body and skin, especially with a BHRP. The BHRP allowed us to obtain high quality Raman spectra of the live animal skin in the totally nondestructive manner. The knowledge on the fat metabolism for body and skin fats and the feasible measuring technique can be used as an alternative intervention for lipid control.

Materials and methods

Animals

Six-week-old Golden Syrian hamsters were obtained (SLC, Shizuoka, Japan). The weight of the hamsters at the beginning of experiment was ranged from 70 to 110 g. All animals (n = 18) were randomly assigned to control or TL- or TC- (TCI, Tokyo, Japan) treated groups. Distilled water for drinking, and TL and TC supplements were newly prepared every day to avoid any kinds of degradation and contamination. The amount of TL and TC supplements were recalculated daily to be approximately 0.5% of each hamster's body weight. Supplements were orally administered between 13:00 and 15:00 hours daily. Picolab Rodent Diet 5053 (LabDiet®, St. Louis, MO, USA) was fed to all treatment groups also. Food and water were available ad libitum, except during oral fat administration. Hamster weight and food intake levels were measured daily to observe abnormalities from oral fat administration. This study was approved by the ethics committee of Kwansei Gakuin University.

Raman measurements

A 785-nm diode laser (Toptica Photonics, Munich, Germany) coupled with a single polychromatic Raman spectrometer (F4.2, focal length 320 mm, 750-nm blazed 600 lines·mm^{-1} grating; Photon Design Co. Ltd., Tokyo, Japan) and a charge coupled device detector (DU420-BRDD; Andor Technology Co. Ltd., Northern Ireland) were used for the Raman measurements (Fig. 1A). For measuring hamster abdominal skin and visceral adipose tissue, the laboratory-made BHRP was used. The probe consisted of a sapphire ball lens 500 μm in diameter (Edmund Optics, USA) and a hollow optical fiber with a 340 μm inner diameter (Doko Engineering LLC, Miyagi, Japan), with a maximum thickness of 640 μm. The BHRP was coupled to the spectrometer through a long-pass filter (LF; Semrock, USA), a notch filter (NF; Kaiser Optical

System, USA), and a coupling lens (CL) to focus the laser into the hollow optical fiber. The spectral resolution was approximately 10 cm^{-1} with a slit-width of 100 μm.

An inhalation anesthesia apparatus (SurgiVet, USA) was used to anesthetize hamsters with 2.0%–2.5% isoflurane (Mylan, Japan). A heating bed (37°C) was used to prevent hypothermia and maintain physiological skin condition. The abdominal region of the hamsters was shaved and cleaned with ethanol (70%). The skin spectra were acquired by two 30-second measurements using a 50-mW excitation light. After skin spectra measurement, hamsters were euthanized using excess isoflurane. The abdominal adipose tissue was then dissected and analyzed. The dissected tissues were stored in -80°C to prevent lipid oxidation.

Lipid oxidation in fatty acids was observed using the same spectrometer described above and the microscope was coupled with an objective lens (×20, N.A. 0.4, Mitutoyo, Japan) in place of the Raman probe. To observe the auto-oxidation of lipids, cis-9, cis-12-18:2 linoleic acid (LA) and cis-9-18:1 oleic acid (OA) were spotted on an open-air dish and kept in a CO_2 incubator (37°C, 100% humidity) for up to 7days. The Raman spectra of these lipids were recorded at 0, 1, 2 and 7^{th} day. The spectrum of trans-10, cis-12-18:2 conjugated LA was also measured with this setup. The structures of LA (a) and conjugated-LA (b) are shown in Fig. 1B. All fatty acid samples were purchased from Sigma-Aldrich (St. Louis, MO, USA).

Data analysis

Raman spectra were corrected for background due to the materials of the sample container; quartz or aluminum, and BHRP. Spectra were then baseline-corrected with a 5^{th} polynomial line fit. The spectra of in vivo skin measurements were then normalized to the phenylalanine band near 1003 cm^{-1} to correct the spectral intensity. The spectra of adipose tissue

and lipid oxidation were normalized using 1440 cm^{-1} of CH_2 band. The areas under the spectra were deconvoluted by Lorentzian curve fitting to estimate the band area. Further spectral processing was carried out using MATLAB (The Mathworks Inc., MA, USA) and Unscrambler (CAMO Software AS., Oslo, Norway).

Results and Discussion

Lipid peroxidation

During the oxidation process, a fatty acid chain is often break down into a peroxide. Lipid peroxidation is involved in many biological processes including lipid degradation, lipid and metabolization.[20] Figure 2 shows the Raman spectra of LA (a) and OA (b) kept in a dark incubator. The spectra were measured at 0, 1, 2, and 7 days and their intensities were corrected with a standard band at 1440 cm^{-1}. Bands at 1655 and 1440 cm^{-1} are assigned to a vinyl C=C stretching mode and C-H deformation modes of the CH_2 and CH_3 groups. The intensity ratio of these bands is often used to evaluate unsaturation in oil products.[15,21] Bands at 1300 and 1264 cm^{-1} are assigned to =C-H and C-H deformation modes of the fatty acid chain. The overlapping spectra of LA show large alterations in its features during the auto-oxidation. A broad band at 865 cm^{-1} is due to the O-OH stretching mode of peroxide. (Supplementary information Fig. S1) Remarkably, the intensity of the band at 1655 cm^{-1} increased over time. This result strongly suggests that the structure of unsaturated LA was transferred from cis-9, cis-12 form to the conjugated form during the initial auto-oxidation process. A Raman spectrum of conjugated-LA is depicted in Fig. 2 (c). It shows a remarkably strong band at 1655 cm^{-1} that is due to a similar C=C stretching mode but indicates conjugated double bonds. These results reveal that the oxidation process was initiated by the dislocation of the double bond in the fatty acid chain. In

the LA spectrum at day 7, a band due to peroxide appeared at 865 cm^{-1} and the band at 1264 cm^{-1} showed reduced intensity, indicating that the double bond was cleaved.[22] Hence, the second oxidation stage occurred following the conjugation process. Furthermore, the band at 1264 cm^{-1} did not increase with the conjugation process and did not resemble the band at 1655 cm^{-1}. This occurs because the hydrogen atom bound to the carbon atom is isolated from the conjugation system. The band intensity did not increase regardless of the structural changes. Hence, the band resulting from the =C-H bending mode is a better marker to evaluate the unsaturation of the lipids than that at 1655 cm^{-1}. The Raman spectra of OA in Fig. 2 (b) shows small changes in contrast to those of LA. Because OA possesses one double bond, trace changes were observed in band intensities at 1655 and 1264 cm^{-1} during the 7 days of auto-oxidation. Besides, the band due to the peroxide group at 865 cm^{-1} did not appear in the spectrum, strongly suggesting that the double bond in the conjugation system is easily oxidized compared with the independent double bond in OA.

It was also reported that the conjugated diene structure was an indicator of early stage lipid peroxidation.[3,4,22,23] The present results are in concordance with the scheme of auto-oxidation in multi-unsaturated lipids. When the lipid has a fatty-acid chain with multiple double bonds, the double bonds require a conjugation system in the chain to reduce the potential energy in the first oxidation process. The conjugated double bonds are rich in π-electrons and the surrounding carbon atoms have a lower density of electrons. This area has a high reactivity and is easily attacked by oxygen, which may be a radical oxygen, to form peroxides, which constitutes the second oxidation process. The peroxyl radical of the lipid can attack its adjacent components including fat or protein membranes.[24] The radical oxygen species (ROS) such as hydroxyl radical and hydroperoxide are prevalently involved in the lipid peroxidation

mechanism. The polyunsaturated fatty acids yield highly susceptible to ROS attack. The ROS reaction comprises 3 steps; initiation, propagation and termination. During the initiation step, the conjugated diene are formed as the hydrogen abstraction occurs. The conjugation system is regarded as an indicator for early stage of lipid peroxidation.[25-28]

Ratios of the band-area intensities of the bands at 1655 and 1264 cm^{-1} ($I_{1655/1264}$) were compared between OA and LA during the auto-oxidation process in Fig. 3A. The overlapping two bands from 1200 to 1350 cm^{-1} were deconvoluted by Lorentzian function curve fitting. The maximum value of $I_{1655/1264}$ was 3.16, which is estimated from the spectrum of the completely conjugated LA (Fig. 2(c)). The minimum value appeared to be 1.12 ± 0.01 for LA and 1.52 ± 0.01 for OA. The difference in these $I_{1655/1264}$ values for OL and OA probably attributes to an overlapping band due to the C=O stretching mode of dimerized LA or OA on the band at 1655 cm^{-1}. The $I_{1655/1264}$ value increased drastically only for LA (up to 2.61 ± 0.28) along with the auto-oxidation. These findings suggest that LA is converted to conjugated-LA. Hence, $I_{1655/1264}$ is a good marker for evaluating the extent of conjugated double bonds produced in the first oxidation process of lipids. Therefore, the band at 865 cm^{-1} is also a good marker for evaluating the peroxidation of lipid produced in the second oxidation process.

The lipid accumulation effect on adipose and skin tissues

Excess dietary-fat intake in rodents and humans was reported to induce mitochondrial H_2O_2 emission, which is the key player of lipid oxidation in skeletal muscle.[29] Kusminski et al. suggested that excess lipid intake can stimulate the mitochondrial electron transport chain (ETC) activity.[30] ETC is a major producer of reactive oxygen species (ROS) in adipocytes, which induce ROS production. According to the studies using 3T3L1-adipocytes, ROS production was

increased when these cells was cultured under high-fat conditions.[31,32] Therefore, the cellular lipid content in the adipocyte is oxidized by ROS and reactive aldehydes, resulting in the production of peripheral components. Previous study has suggested that the adverse effect of dietary fat is not only obesity but also the side-effects resulting from the fat oxidation, which should also be considered.[33]

In this study, the dissected adipose tissue were measured directly in contact with a BHRP. Working distance and sampling volume of the BHRP are 58 μm and 46 μm (FWHM), respectively. [16,17] The sampling volume of BHRP, which was ~50 μm in diameter, is much larger than the size of the cell, suggesting that the spectrum represents the adipose tissues well. The mean spectra of adipose tissues isolated from the controls, TC-, and TL-fed groups measured at the 6th week are depicted in Fig. 4(a). There is no sharp band observed at 1003 cm^{-1} due to phenylalanine which is characteristic for protein. The spectra mostly arise from lipids, suggesting that it is possible to ignore the effect of protein and any other tissue materials in the following analysis. The spectral intensities were corrected with a standard of the band at 1440 cm^{-1} because it represents the total amount of organic materials in the sample. The spectra show a band at 1742 cm^{-1} due to the C=O stretching mode of the ester group in the TG component. Bands at 1655, 1440, and 1264 cm^{-1} are assigned to the C=C stretching mode, C-H bending mode of CH_2 and CH_3 groups, and =C-H bending mode. The subtracted spectra (Supplementary information Fig. S2) of the fat-fed groups and control group showed small bands at the 1655 and 1264 cm^{-1}. They are in positive and negative direction in the difference spectra of the TL- and TC-treated samples, respectively. This finding indicates a reduction and increase in the total number of C=C bonds in the adipose tissue of TC- and TL- fed animals, respectively; however, the difference was too small to discuss in detail with regard to the subtracted spectra. The $I_{1655/\ 1264}$ value of

these spectra are compared in Fig. 3B, which does not show any significant difference up to 6 weeks, suggesting that the oxidation process of lipids proceeds in a remarkably slow manner in adipose tissue. ROS scavengers, such as carotenoids and vitamin E, may reduce lipid oxidation.[22]

The spectra measured in the hamster skin of the control, TC-, and TL-groups are depicted in Fig. 4(b). A band at 1655 cm^{-1} is assigned to an amide I mode of protein, which is much broader than the band due to C=C stretching mode of lipids. Bands arising due to protein are observed at 1263 and 1003 cm^{-1}, which are attributed to the amide III mode and phenyl ring mode of phenylalanine. Strong features appearing from 800 to 950 cm^{-1} are assigned to the proline and C-C skeletal modes of collagen and keratin. It should be noticed that the bands in 1655 cm^{-1} region can be assigned to both C=C and amide I modes as both of which are overlapped. The Raman spectra measured from the stratum corneum was reported to yield composition of ceramide.[34] However, the band at 1742 cm^{-1} assigned to TG is faintly observed in the skin spectra, indicating that the spectra have contribution from TG rather than ceramide. The main producer of TG in the skin is the sebaceous gland, which is resided in the dermis layer of the skin. This suggests the working distance of BHRP deep down into the dermis layer.[16,17]

Chemometrics analysis

We employed PCA to analyze the spectral changes in detail. Partial least square regression (PLSR) analysis was also used for supporting the PCA results. To investigate adipose tissue in detail, all the spectra (n = 135) obtained from 18 animals (control: 6; TC: 6; TL: 6) were subjected to PCA. Figure 5 shows PC1 scores (A) of each sample and loading plots (B) of the PC1. Judging from the spectral feature of the PC1 loading plot, PC1 mainly represents the unsaturation of fatty-acid chains. It shows strong positive bands at 974, 1264 and 1655 cm^{-1},

which are assigned to vibrational modes of double bonds. At the 2nd week, there are no obvious differences observed in the score plot between the datasets for control, TC-, and TL-fed tissues. Along with the term of feeding, the dataset of the TC group has lower, while that of the TL group has higher PC1 scores than the control. This clearly suggests that dietary fat is accumulated directly in adipose tissues. We assigned -1, 0, and 1 for dependent variables of the TC, control, and TL datasets of 6th week and calculated a PLSR-discrimination model. The R square value for leave-one-out cross validation was more than 0.96 for the model constructed only with the factor 1. The loading plot of the factor 1 (Supplementary information Fig. S3) is very similar to that of the PC1. Thus, implying that the accumulation of dietary fat results in a much larger perturbation than that due to individual synthetic lipid characters. Factor 2 seemed to reflect the frequency shift of the bands, which may be attributed to the transformation between trans- and cis- forms of the double bonds. These changes are presumably due to the difference in chain length of TL and TC.

Interestingly, TC (MCFA) is reported to be primarily modified by β-oxidation and be taken into the metabolic lipid circulation rather than accumulated in adipose tissue.[5,6] However, the present result suggests that a relatively large portion of the dietary TC can be stored in the body adipose tissue, which can affect the total amount of TG. Although less than 10 % of MCFA in the post-prandial stage is incorporated into chylomicron-tryglyceride, the adipose tissue preferentially uptake the fatty acids via the chylomicron-triglyceride.[35,36] The accumulation of TC in adipose tissue was found solely in the TC-treated group, that is also confirmed by gas chromatography. (Supplementary information Fig. S4). The present results confirmed that TC cannot be synthesized in the body but the ingested TC can be accumulated in the body.

The Raman spectra of the skin of hamsters fed TL and TC are compared with the control spectra using PCA. The PC1 scores are plotted against the sample number in Fig. 6A-C and their loading plots are shown in Fig. 6D. Because the spectral intensity was standardized with the band at 1003 cm^{-1} owing to the phenylalanine group of protein, a very small contribution from protein is observed in the loading plots and the spectral changes are largely due to the variation in the lipid concentration of the skin sample. Indeed, the features of the PC1 loading plots are similar to that of the adipose tissues in Fig. 4(a). The spectral features of TG are concealed behind the strong contributions of other major components such as protein, making it difficult to analyze the lipid oxidation directly in the original skin spectra (Fig. 4(b)). However, the explained variances of PC1 are 54%, 46%, and 78%, suggesting that the lipid composition in skin is strongly influenced by body fat composition. The $I_{1655/1264}$ values calculated for the PC1 loading plots (Fig. 6E) increased slightly with the feeding terms, suggesting that the conjugation process proceeds on the skin surface in a time-dependent manner. According to the PLSR-discrimination analysis, R square values for the model and leave-one-out cross validation results were 0.22 and 0.18, respectively, for the model obtained with only factor 1. (Supplementary information Fig. S5) The low R square values imply that the composition of sebum does not have a simple linear relation with the dietary fats. Wax esters which account for approximately 25 % of sebum lipids are synthesized only by sebocytes.[37] It suggests that the sebum lipid has a higher content of synthesized fat chains by sebocytes. On the other hand, the variance of the TC or TL dataset is smaller than that of control dataset in the score plot for the dataset of 6^{th} week in Fig. 6C. It suggests that sebocytes in sebaceous gland prefer to capture fatty acids directly from blood and/or lymph, although they are capable of synthesizing various TGs. The loading plot of factor 1 in PLSR analysis showed a large contribution of lipid but was not similar to that of PC1.

The loading plots of factor 2 and 3 had contribution of collagen and/or keratin in 700-850 cm^{-1} region, which may suggested the relation between fat accumulation and hyperkeratinization.[38] Makrantonaki et al. suggested that an increased dietary fat consumption can modify the composition of sebum from sebaceous gland.[39] The sebaceous gland releases sebum through the follicular duct to the uppermost skin layer, where several factors can induce the lipid oxidation including *Propionibacterium acnes*, UV exposure, or natural ROS.[40-44] The present findings and the previous studies suggest that skin lipids become more sensitive to the oxidation process than the body adipose tissue as hamsters grow older.

Conclusion

The present results suggest that dietary fat intake correlates strongly with lipid composition in adipose tissue and on the skin. Analysis of skin lipids gives information about lipid accumulation within the body and individual dietary habits. The present study also demonstrates that Raman spectroscopy with a BHRP is a powerful tool to non-invasively analyze skin lipid composition. It is generally accepted that unsaturated fat is sensitive to lipid peroxidation. Raman spectral analysis of lipid auto-oxidation clearly indicates that multi-unsaturated lipids, such as LA, are converted to conjugated unsaturated structures during early-stage oxidation and then proceed to the peroxidation process. Therefore, the oxidation rate of LA was comparatively higher than that of OA. The area ratio of the bands at 1655 and 1264 cm^{-1} ($I_{1655/1264}$) was a good marker to monitor the formation of the conjugation system in multi-unsaturated lipids, and the peroxide band at 865 cm^{-1} was a marker band for lipid oxidation. These findings were then applied during analysis of lipid accumulation in the adipose tissue and skin of hamsters fed a high saturated fat (TC) and multi-unsaturated fat (TL) diet. Results

showed that conjugated unsaturated lipids increased in the skin and adipose tissue of the hamster over time. The accumulation of TC (MCFA) in adipose tissue was observed only in the TC-treated group, suggesting that TC cannot be synthesized in the body but the ingested TC can be accumulated in the body. PCA results suggested lipid accumulation in skin as well as body adipose tissue originated from dietary fat. The change in lipid accumulation affected not only fat density but also the lipid oxidation process within adipose tissue.

Figure Captions

Fig. 1. Schema of the Raman system (A). It comprises a ball lens-installed hollow optical fiber Raman probe (BHRP), coupling lenses (CL), Long-pass filter (LF), and notch filter (NF). Structures of cis-9, cis-12 (a) and trans-10, cis-12 (conjugated; b) LA are depicted in figure (B).

Fig. 2. Overlapping spectra of LA (a), and OA (b) measured under auto-oxidation at 0, 1, 2, and 7^{th} day, and a spectrum of the fully conjugated LA (trans-10, cis-12; c)

Fig. 3. $I_{1655/1264}$ values of OA and LA under auto-oxidation at 0, 1, 2, 7^{th} days are shown in graph A. The $I_{1655/1264}$ values are also calculated for control, OA-, and LA-fed hamsters measured at 2, 4, and 6 weeks (B).

Fig. 4. The overlapping spectra of adipose (a) and skin (b) tissues measured for control, TC-, and TL-fed hamsters.

Fig. 5. PCA score plots (A) for PC1 of adipose tissue datasets obtained from TC, control TL treated hamsters at 2, 4 and 6^{th} weeks. Loading plots of PC1 and 2 are depicted in (B).

Fig. 6. PCA score plots for PC1 of skin tissues obtained from control (■), TC (○)-,and TL (△)-treated hamsters at 2 (A), 4 (B), and 6 (C) weeks. Loading plots of PC1s (D) depicted for 2^{nd} (a), 4^{th} (b), and 6^{th} (c) week and the $I_{1655/1264}$ values (E) calculated from the loading plots.

References

1. Food and Agriculture Organization of the United Nations (FAO), *FAO Food Nutr Pap.,* 2010, **91**, 1-166
2. L. Hooper, C. D. Summerbell, J. P. Higgins, R. L. Thompson, G. Clements, N. Capps, S. Davey, R. A. Riemersma and S. Ebrahim, *Cochrane Database Syst. Rev.*, 2001, **3**, CD002137
3. S. Ilic, L. Jovanovic and D. J. Pettitt*, Am. J. Perinatol.*, 1999, **16**, 489-495
4. A. G. Dulloo, M. Fathi, N. Mensi and L. Girardier*, Eur. J. Clin. Nutr.*, 1996, **50**, 152-158
5. B. Marten, M. Pfeuffer and J. Schrezenme, *Int Dairy J.*, 2006, **16**, 1374-1382
6. A. A. Papamandjaris, D. E. MacDougall and P. J. Jones, *Life Sci.*, 1998, **62**, 1203-1215
7. G. L. Crozier, *J. Nutr.*, 1988, **118**, 297-304
8. G. H. Johnson and K. Fritsche, *J. Acad. Nutr. Diet*, 2012, **112**, 1029-1041
9. D.B. van Schalkwijk, W.J. Pasman, H. F. J. Hendriks, E. R. Verheij, C. M. Rubingh, K. van Bochove, W. H. J. Vaes, M. Adiels, A. P. Freidig, A. A. de Graaf, *PLoS One*, 2014, **9**, e100376
10. P. J. Caspers, G. W. Lucassen and G. J. Puppels, *Biophys. J.*, 2003, **85**, 572-580
11. A. Tfayli, D. Jamal, R. Vyumvuhore, M. Manfait and A. Baillet-Guffroy, *Analyst*, 2013, **138**, 6852-6858
12. R. Vyumvuhore, A. Tfayli, O. Piot, M. Le Guillou, N. Guichard, M. Manfait and A. Baillet-Guffroy, *J. Biomed. Opt.*, 2014, **19,** 111603
13. J. R. Beattie, S. E. Bell, C. Borggaard, A. M. Fearon and B. W. Moss, *Lipids*, 2007, **42,** 679-685
14. J. R. Beattie, S. E. Bell, C. Borgaard, A. Fearon and B. W. Moss, *Lipids*, 2006, **41**, 287-

294

15. B. Muik, B. Lendl, A. Molina-Díaz and M. J. Ayora- Cañada, *Chem Phys Lipids*, 2005, **134**, 173-182

16. Y. S. Yamamoto, Y. Oshima, H. Shinzawa, T. Katagiri, Y. Matsuura, Y. Ozaki and H. Sato. *Anal Chim Acta*, 2008, **619**, 8-13

17. T. Katagiri, Y. S. Yamamoto, Y. Ozaki, Y. Matsuura and H Sato, *Appl. Spectrosc.*, 2009, **63**, 103-107

18. A. Taketani, R. Hariyani, M. Ishigaki, B. B. Andriana and H. Sato. *Analyst*, 2013, **138**, 4183-4190

19. K. N. Frayn, P. Arner and H. Yki-Järvinen, *Essays Biochem.*, 2006, **42**, 89-103

20. C. D. Funk, *Science*, 2001, **294**, 1871-1875

21. Y. Y. Huang, C. M. Beal, W. W. Cai, R. S. Ruoff and E. M. Terentjev, *Biotechnol. Bioeng.*, 2009, **105**, 889-898

22. F. P. Corongiu and S. Banni, *Methods Enzymol.*,1994, **233**, 303-310

23. R. O. Recknagel and E. A. J. Glende, *Methods Enzymol.*, 1984, **105**, 331-337

24. V. Lobo, A. Patil, A. Phatak and N. Chandra, *Pharmacogn. Rev.*, 2010, **4**, 118-126

25. E. Cadenas and L. Packer, *Handbook of Antioxidants*, Marcel Dekker Inc., New York, 2002. pp. 74-230

26. C. M. Spickett, I. Wiswedel, W. Siems, K. Zarkovic and N. Zarkovic, *Free Radic Res.*, 2010, **44**, 1172-202

27. A. Ayala, M. F. Muñoz and S. Argüelles, O*xid Med Cell Longev,* 2014, **2014**, 360438

28. A. S. Bickerton, R. Roberts, B. A. Fielding, L. Hodson, E. E. Blaak, A. J. Wagenmakers, M. Gilbert, F. Karpe and K. N. Frayn, *Diabetes,* 2007, **56**, 168-76

29. K. Charradi, S. Elkahoui, F. Limam and E. Aouani, *J. Physiol. Sci.*, 2013, **63**, 445-455

30. C. M. Kusminski and P. E. Scherer, *Trends Endocrinol. Metab.*, 2012, **23**, 435-443

31. Y. Lin, A. H. Berg, P. Iyengar, T. K. Lam, A. Giacca, T. P. Combs, M. W. Rajala, X. Du, B. Rollman, W. Li, M. Hawkins, N. Barzilai, C. J. Rhodes, I. G. Fantus, M. Brownlee and P. E. Scherer, *J. Biol. Chem.*, 2005, **280**, 4617-4626

32. X. H. Chen, Y. P. Zhao, M. Xue, C. B. Ji, C. L. Gao, J. G. Zhu, D. N. Qin, C. Z. Kou, X. H. Qin, M. L. Tong and X. R. Guo, *Mol. Cell Endocrinol.*, 2010, **328**, 63-69

33. L. K. Philp, L. K. Heilbronn, A. Janovska, G. A. Wittert, *PLoS One*, 2015, **10**, e0117494

34. P. D. Pudney, E. Y. Bonnist, P. J. Caspers, J. P. Gorce, C. Marriot, G. J. Puppels, S. Singleton and M. J. van der Wolf, *Appl. Spectrosc.*, 2012, **66**, 882-891

35. Y. Q. You, P. R. Ling, J. Z. Qu and B. R. Bistrian, *JPEN J Parenter Enteral Nutr.,* 2008, **32**, 169-75

36. J. E. Lambert and E. J. Parks, *Biochim Biophys Acta,* 2012, **1821**, 721-6

37. A. Pappas, *Dermatoendocrinol.*, 2009, **1**, 72-76

38. W. J. Lee, H. D. Jung, S. G. Chi, S. B. Kim, S. J. Lee, W. Kim do, M. K. Kim and J. C. Kim, *Arch Dermatol Res.* 2010, **302**, 429-33

39. E. Makrantonaki, R. Ganceviciene, and C. Zouboulis, *Dermatoendocrinol*, 2011, **3**, 41–49.

40. T. Tochio, H. Tanaka, S. Nakata and H. Ikeno, *J. Cosmet. Dermatol.*, 2009, **8**, 152-158

41. G. F. Vile and R. M. Tyrrell, *Free Radic. Biol. Med.*, 1995, **18**, 721-730

42. J. Lasch, U. Schönfelder, M. Walke, S. Zellmer and D. Beckert, *Biochim. Biophys. Acta.*, 1997, **1349**, 171-181

43. C. S. Sander, H. Chang, S. Salzmann, C. S. Müller, S. Ekanayake-Mudiyanselage, P.

Elsner and J. J. Thiele, *J. Inv. Derm.*, 2002, **118**, 618-625

44. L. Hodson, C. M. Skeaff and W. A. Chisholm, *Eur. J. Clin. Nutr.*, 2001, **55**, 908-915

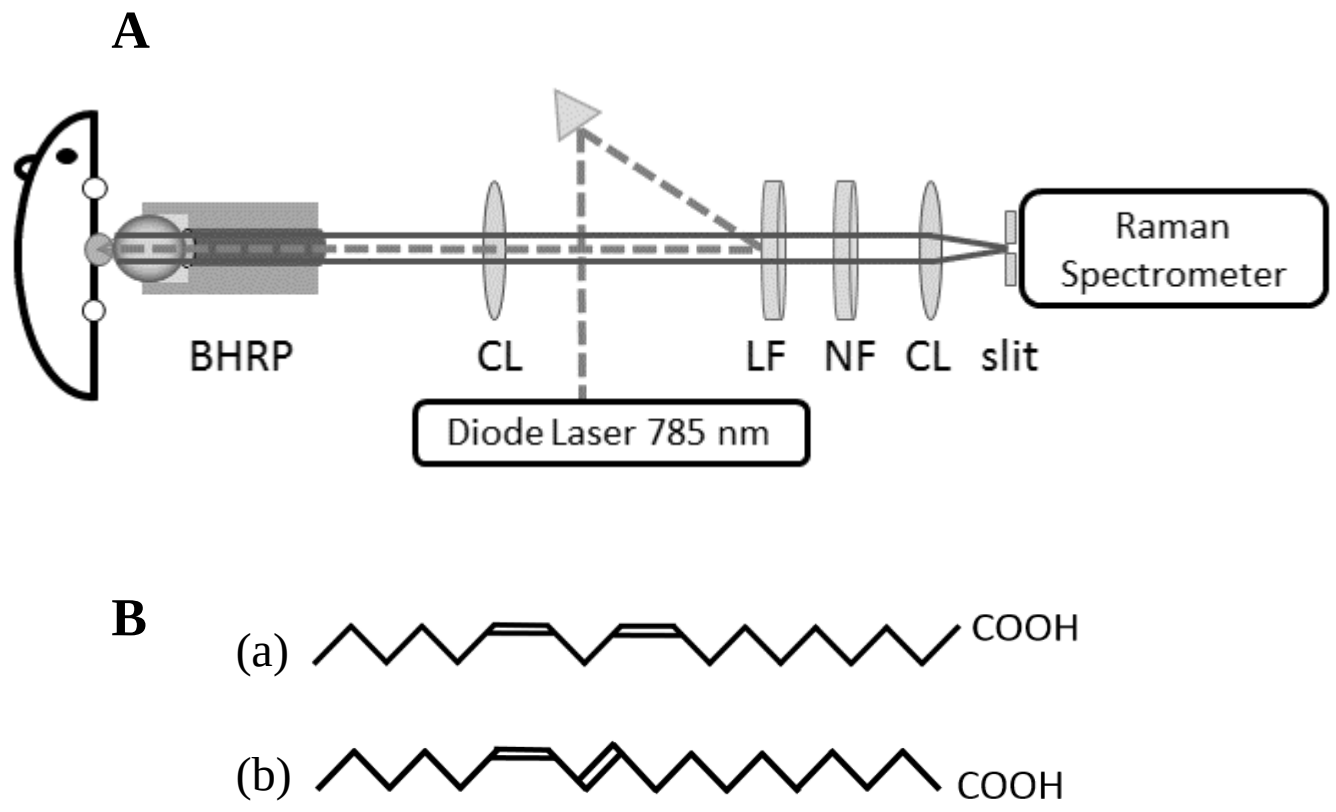

Fig. 1

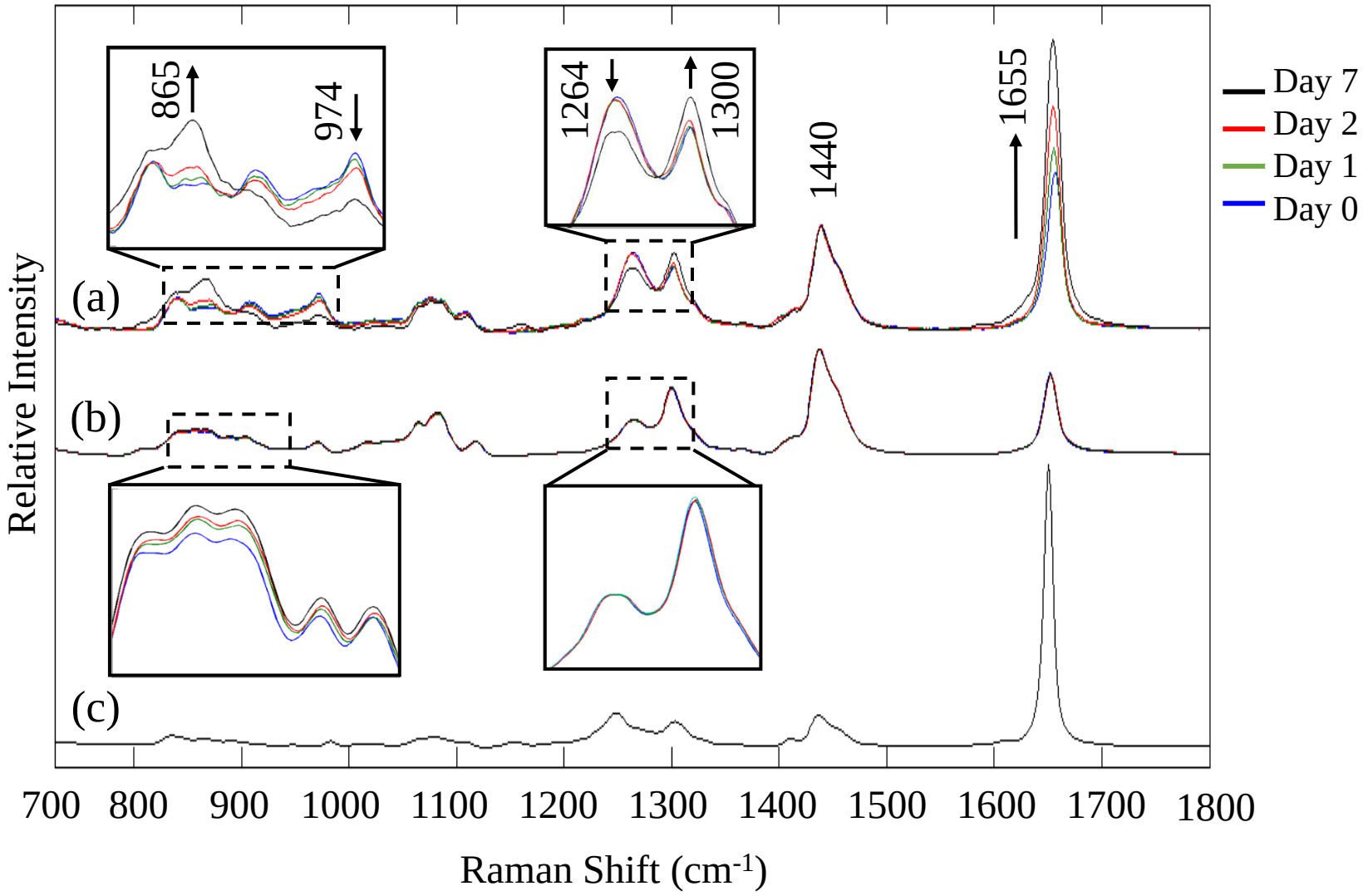

Fig. 2

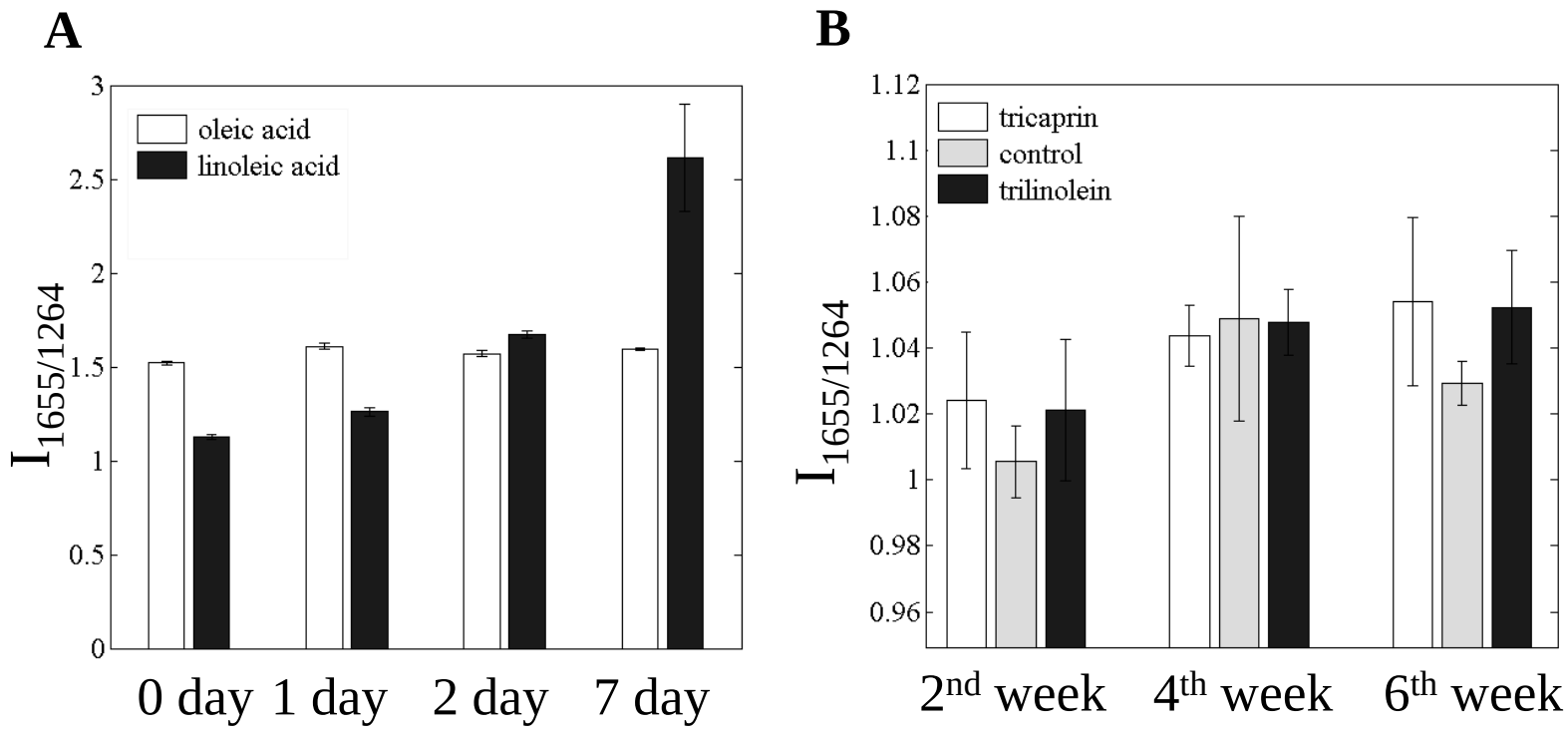

Fig. 3

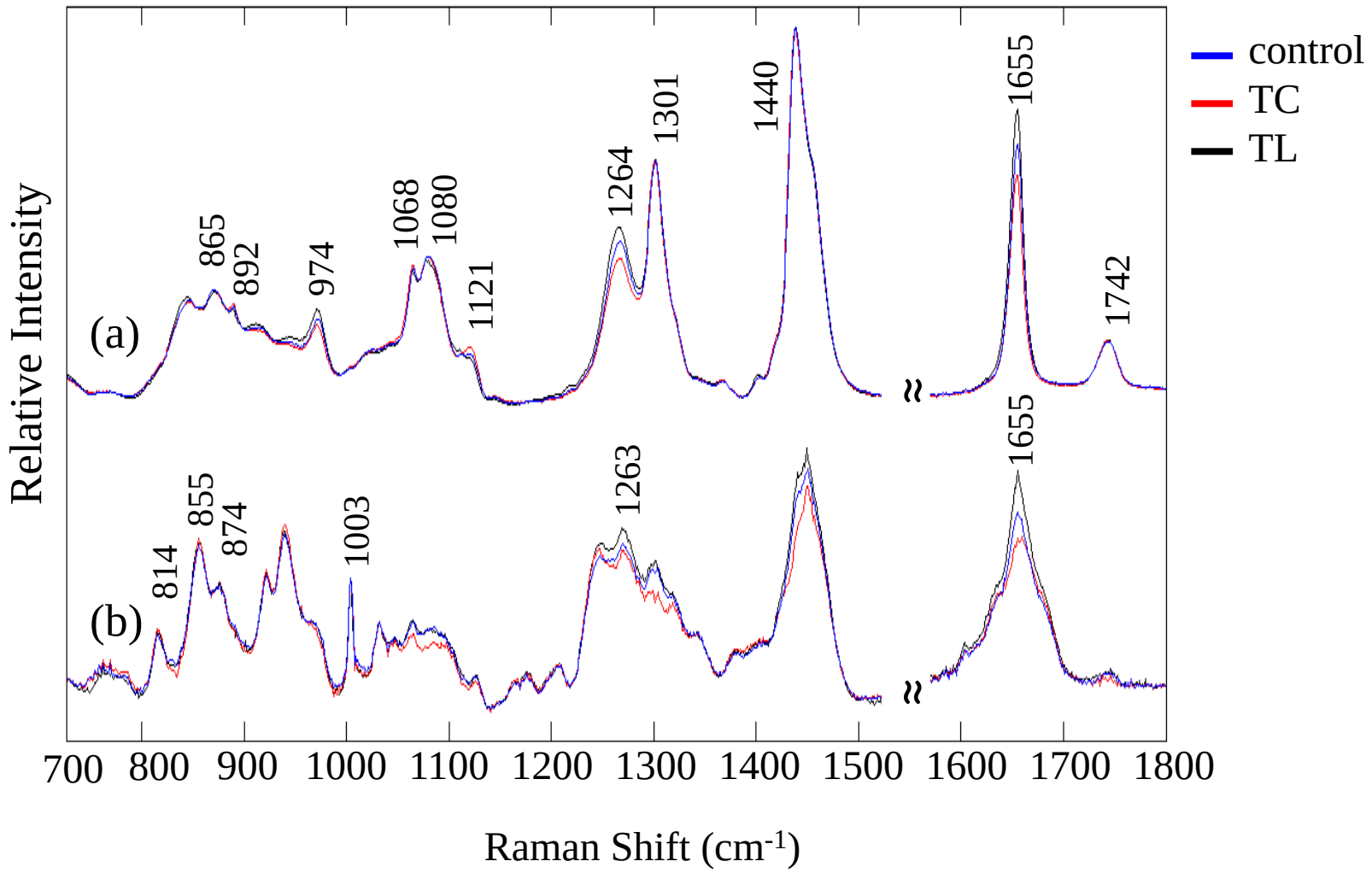

Fig. 4

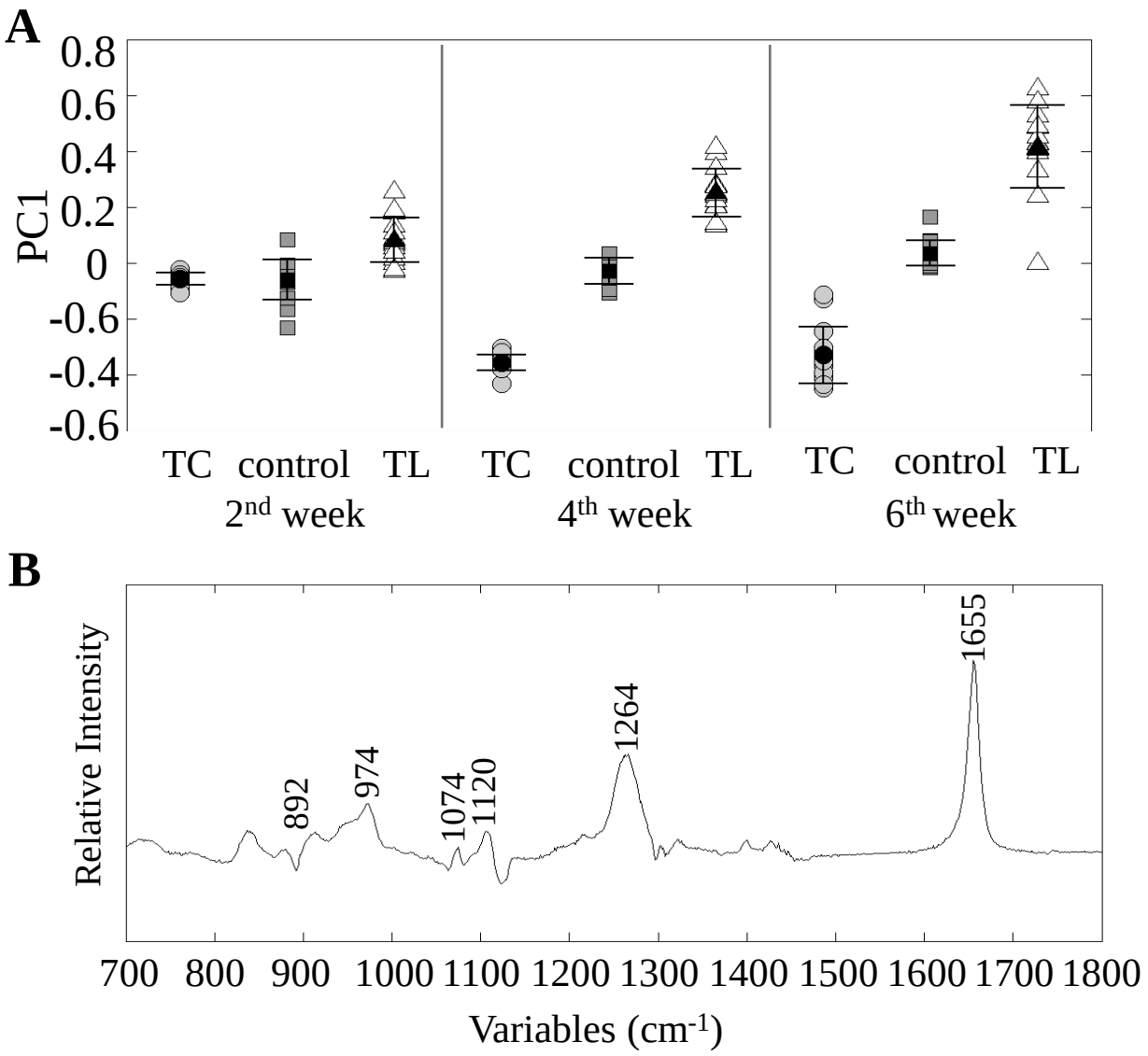

Fig. 5

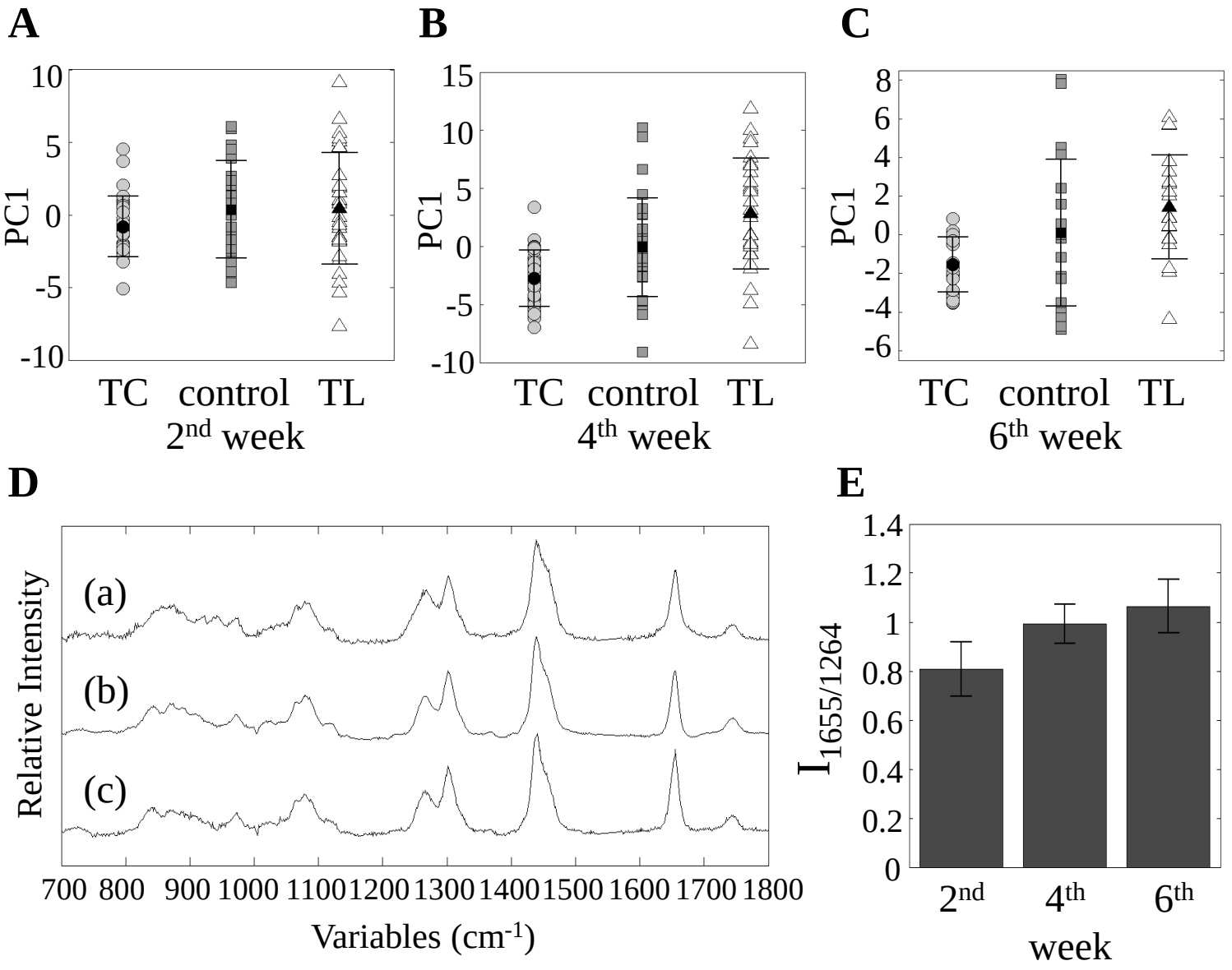

Fig. 6